Design and Analysis of a New Zero Current Transition Bidirectional DC-DC Converter for Energy Storage Systems

Pramod Kumar Aylapogu[1,2], Veera Venkata Subrahmanya Kumar Bhajana[1,2], Pavel Drabek[2], Martin Jara[2]
[1]*School of Electronics Engineering, KIIT University, Campus-12, Bhubaneswar-751024, Odisha, India*
[2]*Regional Innovation Centre for Electrical Engineering, University of West Bohemia, Pilsen 30614, Czech Republic*
aylapogu.pramodkumar@gmail.com

***Abstract*—This paper proposes a new zero-current transition based non-isolated bidirectional DC-DC converter for battery storage appliances in DC traction vehicles. The proposed converter has an auxiliary IGBTS, auxiliary inductor, auxiliary capacitor and bypass diodes are additionally to the main converter module. Usually, the zero-current transition achieved for the main IGBTs circuit has major advantages like reduced turn-off losses, overall conduction losses and minimized reverse recovery problems to the anti-parallel diodes of the main IGBTs. The operation principles, simulation and experimental investigations on 150 V/250 V/1 kW laboratory prototype are presented in order to show the performance and also to verify the soft-switching characteristics in boost/buck modes of the converter.**

***Index Terms*—Zero current transition; DC-DC; Bidirectional; Energy storage systems.**

I. INTRODUCTION

Bidirectional DC-DC converters play a very important role in energy storage systems in DC traction vehicles (Electric Vehicles e.g. battery operated). Industry demands on lossless efficient converters for storage systems in electric vehicles. Soft-switching is the only way to produce efficient converters. There is a lot of research focuses on achieving zero-voltage switching / zero-current switching operations using the resonant auxiliary circuits to the non-isolated bidirectional DC-DC converters. Zero-voltage switching based converter [1] has been developed to achieve soft-turn on with the aid of resonant cell incorporated with the main converter. Those converters may have poor efficiency and more conduction losses due to very lower input voltages and power levels. Zero-current switching cell has been introduced [2] for PWM DC-DC converters with the aid of more resonant elements to the main IGBTs, which increases the cost and additional losses of the auxiliary circuit that may degrade the efficiency of the converter. An isolated flyback dc-dc converter [3] has been developed with the simple auxiliary circuit, operated at very low voltage levels. A low power DC-DC converter with two switch flyback converter [4] tested under microinverter and electrical grid loads. It has operated under hard-switching condition and achieved the poor efficiency at low output power. Generally, for isolated circuit operated at low input levels, the switching power losses may not be considered. A non-isolated boost converter [5] switching devices obtained soft-commutation for both turn-on and turn-off conditions. This soft-commutation achieved with the aid of auxiliary switch, coupled inductor and snubber circuits. This may increase the cost relatively and also it has a drawback in auxiliary switch frequency which is twice of the main operation frequency. Various zero-current transition bidirectional converters [6] have been introduced with auxiliary cells, are operated under low power and obtained marginal efficiency. A buck converter has also been implemented with zero-current transition [7] with the help of an auxiliary circuit along with coupled inductor. Another soft-switching bidirectional converter [8] was implemented with the complex resonant circuit; however, the device count is increased. As per the previously published work of non-isolated converters [9], [10], soft-switching operations have been achieved with nominal efficiencies. Therefore, the industry needs high efficient converters with reduced device count and reduced switching stresses. Nowadays, there are many converters have been implemented with coupled inductors, auxiliary resonant circuits and snubber cells. But as of now, they didn't achieve the affective results on non-isolated bidirectional converter that must be operated at some higher power-levels. The main aim of this paper is to propose a new design on non-isolated bidirectional converter with the main features of soft-commutation and low turn-on/off current stresses on main switches. The other major advantages are, that has a simple auxiliary resonant circuit to reduce the switching and conduction losses for a different input voltage ranges. The overall structure of the energy storage system in DC traction is presented in Fig. 1. The overhead lines supply (DC 450 V–600 V) which is directly connected with traction

Manuscript received 3 January, 2018; accepted 19 May, 2018.
This research has been supported by the Ministry of Education, Youth and Sports of the Czech Republic under the RICE – New Technologies and Concepts for Smart Industrial Systems, Project No. LO1607.

motor and the same voltage is connected with auxiliary power supply systems. The auxiliary power supply delivers the power via isolated full bridge converter and the other side of this battery storage system is connected via the bidirectional converter, which is normally non-isolated. In general, the batteries use the SC (Super capacitors), Fuel cells, etc.

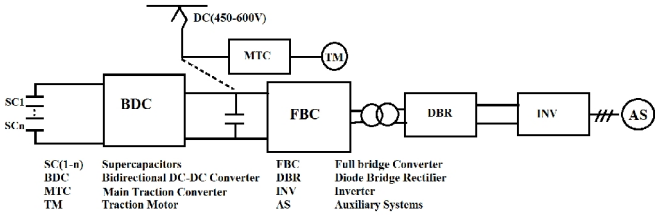

Fig. 1. Structure of energy storage system: DC traction.

II. CONVERTER TOPOLOGY

Figure 2 shows the proposed converter. Basically, it operates in two modes. The first is boost mode, which means that the battery will deliver the power to the next stage (i.e. Full bridge converter). And the other mode is a buck mode where the battery gets charged that will be provided by the bidirectional converter. In boost mode, the converter main switches S_2 and S_1 are in conducting and turned-off, respectively. When the converter operates in buck mode, the S_1 is to be gated and it is used to transfer the output power. During this mode, S_2 is in turn-off throughout the operation.

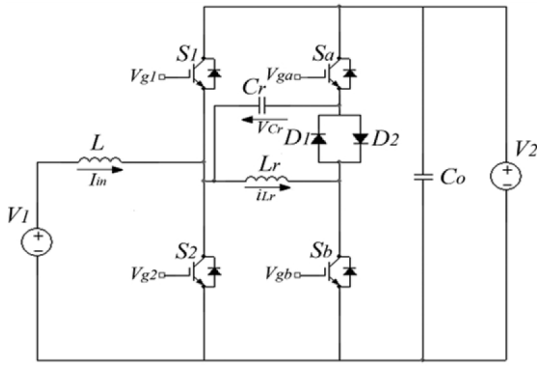

Fig. 2. Proposed ZCT bidirectional DC-DC converter.

The proposed converter is also included the auxiliary resonant circuit to provide the soft-commutation of the main switches (S_1, S_2). The passive devices in the auxiliary circuit are one auxiliary inductor (L_r) and an auxiliary capacitor (C_r). The active devices present in the topology are two auxiliary IGBTs S_a, S_b and two bypass diodes D_1, D_2. The Table I shows the gated and conducting devices in the boost and buck modes.

TABLE I. GATED AND CONDUCTED DEVICES.

Interval	Mode of operation	Gated	Right leg Conducted	Left Leg Conducted
t_0-t_1	Boost mode	S_2	S_2	Body diode of S_b
t_1-t_2	Boost mode	S_2,S_b	S_2	S_b
t_2-t_3	Boost mode	S_b	0	S_b
t_3-t_4	Boost mode	S_b	Body diode of S_2	S_b
t_4-t_5	Boost mode	*0*	0	0
t_5-t_6	Boost mode	*0*	0	0
t_0-t_1	Buck mode	S_1	S_1	Body diode of

Interval	Mode of operation	Gated	Right leg Conducted	Left Leg Conducted
				S_a
t_1-t_2	Buck mode	S_1,S_a	S_1	S_a
t_2-t_3	Buck mode	0	0	S_a
t_3-t_4	Buck mode	S_a	Body diode of S_1	S_a
t_4-t_5	Buck mode	*0*	*0*	*0*
t_5-t_6	Buck mode	*0*	0	0
t_0-t_1	Boost mode	S_2	S_2	Body diode of S_b
t_1-t_2	Boost mode	S_2,S_b	S_2	S_b
t_2-t_3	Boost mode	S_b	0	S_b
t_3-t_4	Boost mode	S_b	Body diode of S_2	S_b
t_4-t_5	Boost mode	*0*	0	0
t_5-t_6	Boost mode	*0*	0	0
t_0-t_1	Buck mode	S_1	S_1	Body diode of S_a
t_1-t_2	Buck mode	S_1,S_a	S_1	S_a
t_2-t_3	Buck mode	0	0	S_a
t_3-t_4	Buck mode	S_a	Body diode of S_1	S_a
t_4-t_5	Buck mode	*0*	*0*	*0*
t_5-t_6	Buck mode	*0*	0	0

III. SWITCHING WAVEFORMS AND ITS STAGES

The theoretical waveforms of the proposed converter are illustrated in Fig. 3. The boost and buck mode operations of this topology are described.

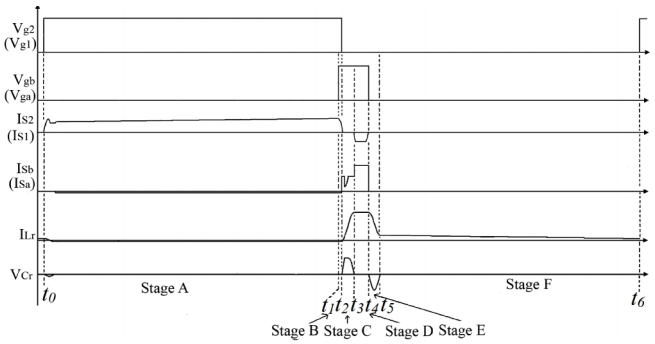

Fig. 3. Key waveforms boost (buck) modes.

A. Boost Mode

The proposed converter's switches can be operated under zero-current transition; the switching waveforms with the aid of gating signals are shown in Fig. 3. The converter soft turn-off operation will be obtained when the auxiliary active device S_b is gated prior to the main switch turning-off. Fig. 4(a)–Fig. 4(e) shows the current flow equivalent schematics of boost mode. The operating stages have been divided into four modes as Energy accumulation stage (Stage A), Auxiliary stage (Stage B), Resonant (Stage C), Freewheel mode (Stage D) and Power transferring (Stage E and Stage F).

Energy Accumulation mode (Stage A): At time t_0 of this stage, the gating signals are applied to the converter main switch S_2 and it starts conducting. Throughout this stage, the energy in the input inductor L gets accumulated via V_1-L-S_2.

Auxiliary stage (Stage B): The gating signals are applied to auxiliary IGBT S_b and S_2 is already being conducted. The resonant inductor and capacitors are in resonating together. At the end of this time interval, the current of the IGBT S_2

reached zero.

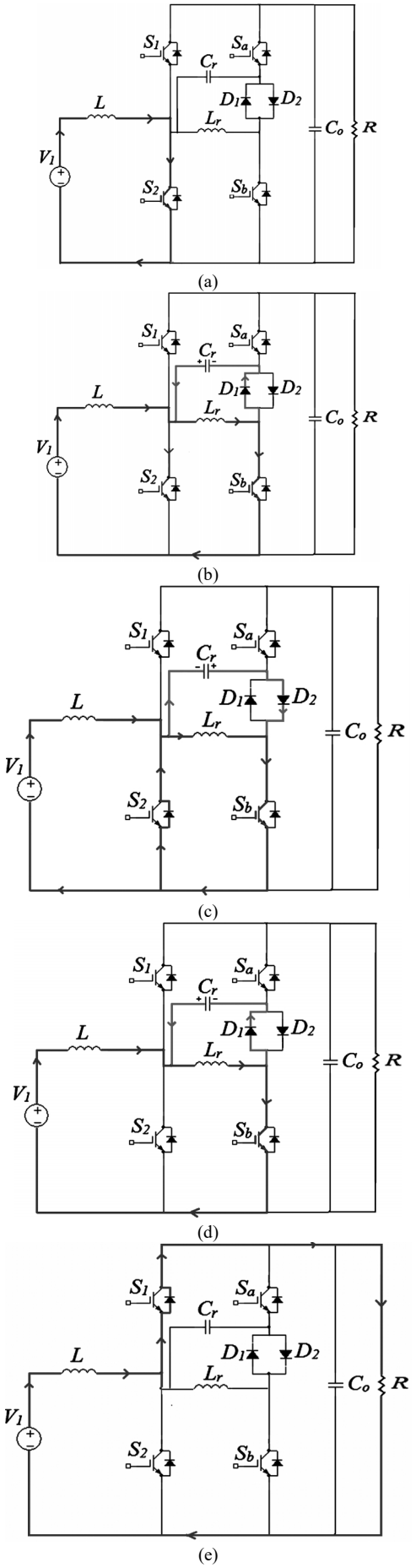

Fig. 4. Stage A (a); Stage B (b); Stage C (c); Stage D (d); Stage E and Stage F (e).

Resonant stage (Stage C): The current of the IGBT S_2 is reached zero, which represents the soft-turn-off and at the same time the resonant current of I_{Lr} is at the peak that equals to the input current of L. Then, the auxiliary capacitor C_r charged to the 1/4th of its input voltage. The resonance time equals to 1/4th of the resonant inductor current L_r. The bypass diode D_1 starts conducting to provide path to flow energy of resonant tank (L_r, C_r).

Freewheeling stage (Stage D): From the beginning of this interval, the main switch S_2 is in turned-off and the auxiliary IGBT S_b is still conducting. The resonant inductor L_r reached to a constant current, which equals to input current. During this stage, the energy stored in capacitor C_r gets discharged through the short-circuited path C_r-D_2-S_b-body diode of S_2, hence the voltage across capacitor C_r is approximately zero.

Power transferring stage (Stage E & Stage F): All the IGBTs are turned off in this mode, accumulated energy of L will be delivered to the output.

B. Buck Mode

In the operation of buck mode, S_1 is the only main IGBT used to transfer the output power and auxiliary IGBT switch S_a will turn-on before the main switch S_1 gets turned-off, in order to obtain zero current transition. Figure 5 shows the equivalent circuit of buck mode.

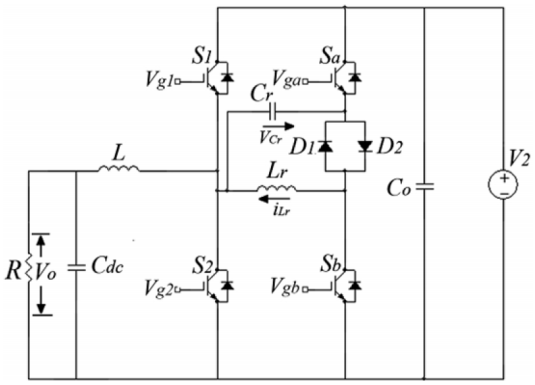

Fig. 5. Buck mode equivalent circuit.

The converter operation has been divided into four modes as, Stage A unlike boost mode (power transferring mode), Stage B (Auxiliary stage), Stage C (Resonating mode), Stage D (Freewheel mode) and Stages E & F as non-conducting mode (Turn-off). The only difference in operation of buck mode is when the main switch S_1 is in conduction, there will be a power at the output during the first stage A. The Stage E operation is exactly opposite to the boost mode of operation. That is, whenever the main switch is turned-off, there is no output power will be delivered. The equivalent current flow schematics for all stages are depicted in Fig. 6(a)–Fig. 6(e).

III. ANALYSIS

The theoretical analysis of the proposed converter is explained in this section by assuming the following:

The input and output voltages are ripple free;

All the active devices are ideal;

Constant switching frequency

From Stage B: The resonant inductor current i_{Lr} and capacitor voltages V_{Cr} are at zero.

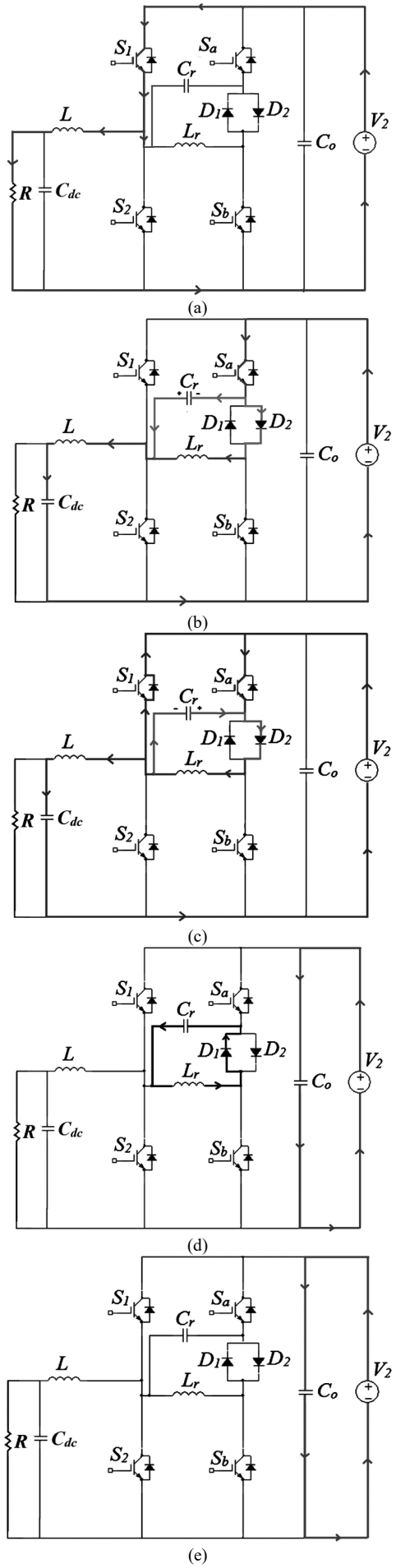

Fig. 6. Stage A (a); Stage B and Stage C (b); Stage D (c); Stage E (d); Stage F (e).

From Stage C (t_2–t_3), the resonant inductor current i_{Lr} and capacitor voltage V_{Cr} expressed as:

$$i_{Lr} = \frac{V_{Cr}}{Z}\sin\omega(t-t_3), \tag{1}$$

$$V_{Cr} = V_{Cr(peak)}\cos\omega(t-t_3). \tag{2}$$

Where characteristic impedance

$$Z = \sqrt{\frac{L_r}{C_r}}, \tag{3}$$

and angular frequency

$$\omega = \frac{1}{\sqrt{L_r C_r}}. \tag{4}$$

After a quarter of this cycle between t_2 and t_3, the capacitor voltage is reached to peak i.e. $V_{Cr(peak)}$ and auxiliary inductor current is also reached to the maximum i.e. $I_{Lr(max)}$. The equations for $V_{Cr(peak)}$ and $I_{Lr(max)}$ can be expressed as:

$$I_{Lr(\max)} = \frac{V_{Cr(Peak)}}{Z}, \tag{5}$$

$$V_{Cr(peak)} = \frac{ZI_{in}}{\cos\left(2\pi T_{aux}/T_x\right)}, \tag{6}$$

where $T_x = 2\pi\sqrt{L_r C_r}$.

T_{aux} = Total time of Turn-on of Auxiliary IGBT.

From Stage E (t_4-t_5): The capacitor voltage V_{Cr} can be expressed as

$$V_{Cr} = -\frac{I_{Lr}}{C_r}\sin\omega(t-t_4). \tag{7}$$

IV. Conditions to Obtain Zero Current Transition

The zero-current transition to the main IGBT would be obtained if the following conditions satisfied:

$$V_{Cr} \le V_o, \tag{8}$$

$$I_{Lr(\max)} \ge I_{in}, \tag{9}$$

where the capacitor voltage V_{Cr} is lesser than the output voltage V_o and maximum current of resonant inductor $I_{Lr(max)}$ must be greater than or equals to input inductor current I_{in}.

In general, the auxiliary inductor $I_{Lr(max)}$ has a maximum current of 10 % which is more than the input inductor current. Based on (6), the time of conducting period can be chosen as 1.29 % of the total conducting period of the main IGBT (S_1 or S_2). Based on (7), the peak voltage of the auxiliary capacitor is about 1/4th of the output voltage, which is equal to nearly 50 V in Boost mode and 25 V in buck mode. If both the conditions of (8) and (9) is satisfied, then the soft-commutation will be obtained while the main IGBT turning-off.

V. SELECTION OF AUXILIARY DEVICES

Auxiliary Inductor (L_r) & Capacitor (C_r): If the value of the resonant inductor L_r is much smaller than the input inductor, the circulating energy of converter is quite small. There will be an energy transfer between the auxiliary elements and to the main active devices only during the period of (t_2-t_4). The resonant frequency and the characteristic impedance of the resonant circuit are chosen as 13 MHz and 8.164 Ω, respectively. So, the auxiliary inductor chosen a very small value of 1 µH and auxiliary capacitor is 15 nF, in order to minimize the circulating energy.

VI. SIMULATION AND EXPERIMENTAL EVALUATIONS OF PROPOSED TOPOLOGY

The computer simulations were performed on the proposed topology based on the simulation parameters used as mentioned in Table II. The topology has been verified for both in boost and buck modes. The soft-commutation of the main IGBT switch S_2 is proved by the results as shown in Fig. 7, where the design simulations are performed for buck mode. Figure 8 shows the currents of the S_1,S_a, L_r ,D_2 and capacitor voltage C_r. The experimental investigations are performed on two different input voltages in boost mode as 100 V and 150 V. In both the cases, the maximum output power of 1 kW for the prototype has been tested to verify the theoretical analysis. Note that the difference of the analysis shown in switching waveforms in Fig. 3 is different from the experimental waveforms due to the non-ideal characteristics of active devices.

TABLE II. COMPONENTS AND PARAMETERS.

Parameters	Symbol	Value
Input voltage	V_1	150 V
Input voltage	V_2	250 V
Maximum output power	P_o	1 kW
Switching frequency	f_{sw}	50 kHz
Input inductor	L	200 µH
Resonant inductor (IHLP-2525CZ-ER-1R0-M-01)	L_r	1 µH
Resonant capacitor (C3216)	C_r	15 nF
Output capacitor	C_o	470 µF
Main switches	$S_{1\text{-}2}$	IKW40H1203

The soft-commutation of the IGBTs S_1 and S_2 are obtained successfully with an additional advantage of very small circulating energy and reverse recovery problem of anti-parallel diode of the main IGBTs (S_1 and S_2). Current stresses are reduced while the main IGBT is being turning-off. The duty cycles used for the main IGBT are chosen as 0.40 for boost mode and 0.78 for buck mode, respectively. Figure 8 shows the measured waveforms for the boost mode, when converter operated at 150 V input and obtained 260 V output voltage with 1 kW output power.

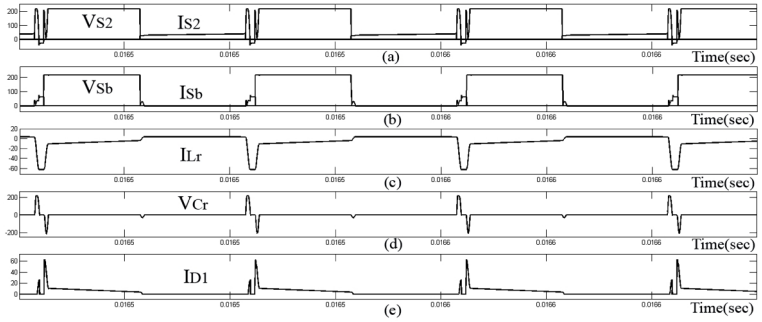

Fig. 7. Simulated results: (a) IGBT S_2 voltage (V_{S2}) and currents (I_{S2}); (b) IGBT S_b voltage(V_{Sb}) and currents (I_{Sb}); (c) resonant inductor current I_{Lr}; (d) resonant capacitor voltage V_{Cr}; (e) diode current (I_{D1}): boost mode.

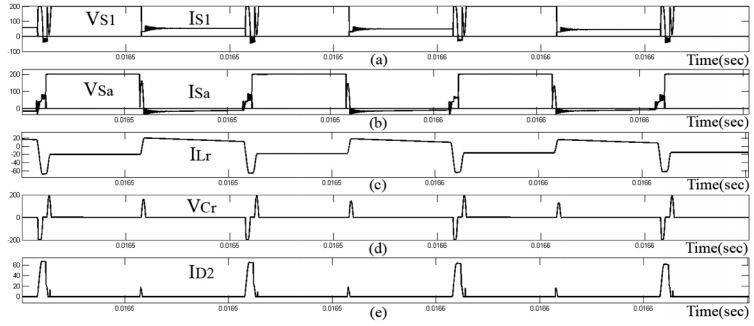

Fig. 8. Simulated results: (a) IGBT S_1 voltage (V_{S1}) and current (I_{S1}); (b) IGBT S_a voltage (V_{Sa}) and current (I_{Sa}); (c) resonant inductor current (I_{Lr}); (d) resonant capacitor voltage (V_{Cr}); (e) diode current (I_{D2}): buck mode.

Figure 9 shows the voltage and currents of IGBT switch S_2 and auxiliary switch S_b. The obtained waveform proves that the soft-commutation of the main switch is achieved while it gets turned-off and it is observed that there is not much negative current passes through the anti-parallel diode. Therefore, that will impose the effect on the reverse recovery problem. Figure 10(a) illustrates the resonant inductor current and capacitor voltage, the average of the inductor current is about 10 A when the converter is operated at 920 W output power. Then the auxiliary capacitor is charged and discharged where the peak-to-peak voltage is about 50 V which is equal to 1/4th of the output voltage. Figure 10(b) shows the diode D_1 current of about 6 A, it is nearly equal to the input current. This diode conduct a very small amount of time, the time of conducting equals to the time of auxiliary switch conduction. The main purpose

of the bypass diodes in this topology is to trap the trapped energy in the auxiliary inductor. Similarly, the experimental investigations were performed for buck mode for the 250 V input voltage and 160 V output voltage with 50 kHz operating frequency. The soft-switching operation is achieved for the main switch S1, when the auxiliary switch S_a is gated before its turn-off. Remaining all the semiconductors are in turn-off condition during this buck mode. Figure 11 shows the measured waveforms of the voltage and currents of the IGBT S_1 and S_a.

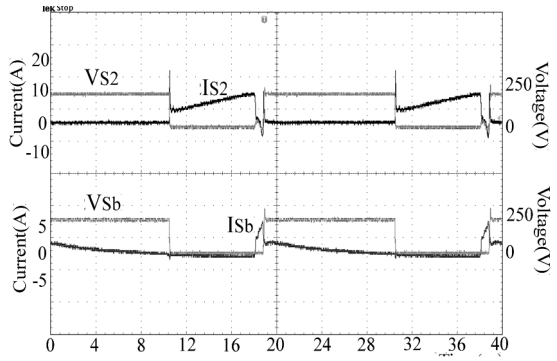

Fig. 9. Experimental waveforms of the converter: boost mode voltage V_{S2} and currents I_{S2} of the IGBT S_2 and auxiliary IGBT S_b.

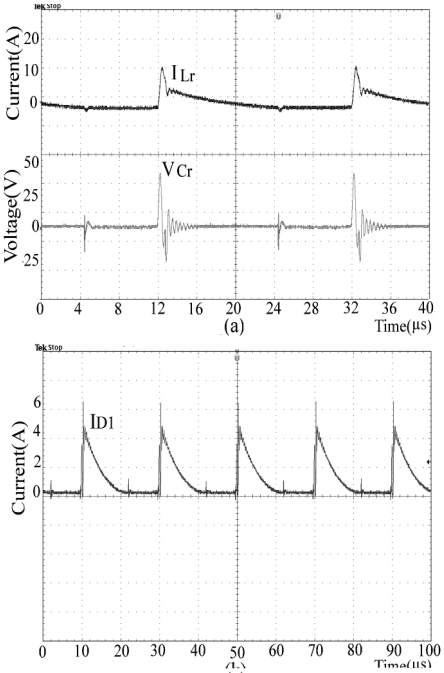

Fig. 10. Measured auxiliary inductor current (I_{Lr}) and auxiliary capacitor voltages (V_{Cr}) (a); measured bypass diode current(I_{D1}): boost mode (b).

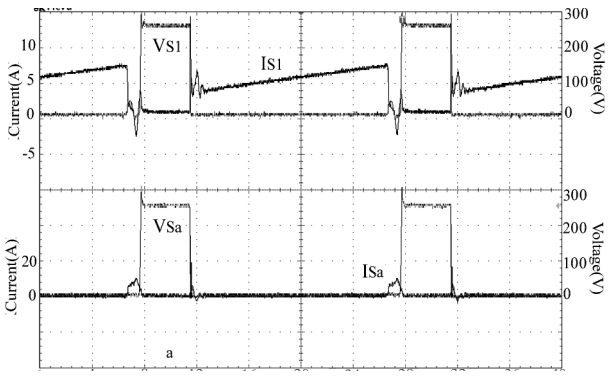

Fig. 11. Measured waveforms for the voltage and currents of the IGBTs(S_1 and S_a): buck mode.

Figure 12 shows the auxiliary inductor's, capacitor's currents and voltages, respectively. Figure 13(a), Fig. 13(b) and Fig. 14(a), Fig. 14(b) show the turn-on and turn-off transitions of main switches (S_1, S_2), auxiliary switches (S_a, S_b) for boost and buck mode, respectively. Based on the obtained experimental results, the switching power losses are reduced, while the main switch is commutating. There are no additional losses by the active devices D_1 and D_2, because these devices will conduct a small portion of the overall switching cycle.

The major advantage is a small amount reverse current flow through the main IGBTs and it will effect on the reverse recovery problem of the both the IGBTs (S_1 and S_2). The efficiencies for the boost and buck modes are the function of output power by input power.

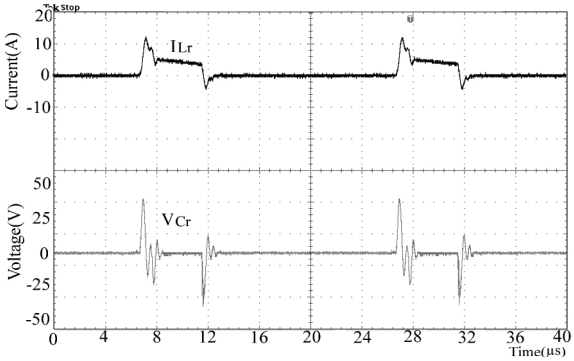

Fig. 12. Measured waveforms for the currents auxiliary inductor (I_{Lr}) and voltage (V_{Cr}) of the auxiliary capacitor: buck mode.

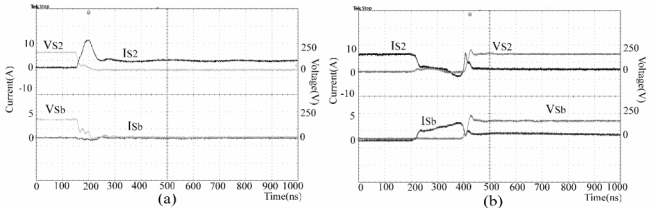

Fig. 13. Turn-on transition of S_2 and S_b (a); turn-off transition of S_2 and S_b: boost mode (b).

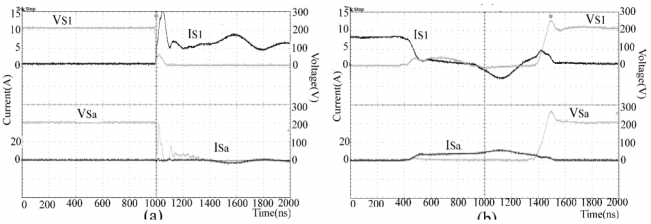

Fig. 14. Turn-on transition of S_1 and S_a (a); turn-off transition of S_1 and S_a: buck mode (b).

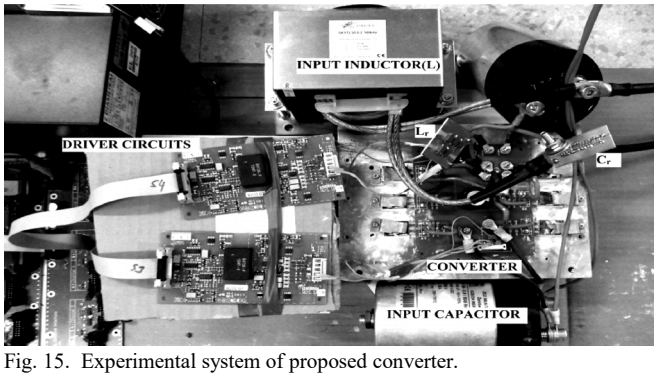

Fig. 15. Experimental system of proposed converter.

The boost mode efficiency of 95.5 % was obtained when

the converter operated at 1 kW output power with 150 V input voltage. The maximum efficiency obtained is 98.5 % at 500 W output power for the 250 V input voltage. The photograph of experimental system of proposed converter is shown in Fig. 15.

The comparison of previous ZCT non-isolated DC-DC converter topologies with the presented topology are given in Table III.

TABLE III. EFFICIENCY COMPARISONS.

Toplogies	Power rating	Efficiency
Topology [2]	1 kW	97.3 %
Topology [3]	30 W	87.5 %
Topology [5]	300 W	98.3 %
Topology [6]	200 W	94.5 %
Presented topology	1 kW	98.5 %

As per the efficiency comparisons, the proposed topology was obtained 98.5 % at maximum output power of 1 kW. whereas previous topologies [2], [3], [5], [6] are operated at low output power level.

VII. CONCLUSIONS

This paper proposed a zero current transition based non-isolated bidirectional DC-DC converter for the battery back-up systems in DC traction. This paper clearly discussed the operating stages, analysis with the help of simulation and experimental verifications. The proposed converter has the maximum efficiency is about 98.5 % in buck mode and 95 % in boost mode, respectively. The soft-switching of the IGBTS were achieved successfully with additional advantages of reduced turn-off losses, minimized reverse recovery problem of anti-parallel diodes of main switches. As from the earlier converters, the present converter seems to be more efficient and lossless. This proposed bidirectional converter has a simple auxiliary resonant, reduced turn-off losses and high efficiency preferable for the energy storage applications.

REFERENCES

[1] E. Adib, H. Farzanehfard, "Soft switching bidirectional DC–DC converter for ultracapacitor batteries interface", *Energy Conversion and Management*, vol. 50, no. 12, pp. 2879–2884, 2009, DOI: 10.1016/j.enconman.2009.07.001.

[2] C. M. Wang, C. H. Su, C. W. Tao, "Zero-current-transition PWM DC-DC converters using new zero-current-switching PWM switch cell", in *Proc. IEE Electric Power Applications*, 2006, vol. 153, no. 4, pp. 503–512. DOI: 10.1049/ip-epa:20050146.

[3] D. Murthy-Bellur, M. K. Kazimierczuk, "Zero-current-transition two-switch flyback pulse-width modulated DC-DC converter", *IET Power Electronics*, vol. 4, no. 3, pp. 288–295, 2011. DOI: 10.1049/iet-pel.2009.0253.

[4] S. Larousse, H. Razik, R. Cellier, "Self-calibrated valley switching for wide range Flyback active-clamp DC-DC converter", in *IEEE 8th Int. Conf. Power Electronics and Motion Control,* 2016, pp. 1134–1138. DOI: 10.1109/IPEMC.2016.7512447.

[5] B. Akin, "An improved ZVT–ZCT PWM DC–DC boost converter with increased efficiency", *IEEE Trans. Power Electronics*, vol. 29, no. 4, pp. 1919–1926, 2014. DOI: 10.1109/TPEL.2013.2269172.

[6] M. Ahmadi, M. R. Mohammadi, E. Adib, H. Farzanehfard, "Family of non-isolated zero current transition bi-directional converters with one auxiliary switch", *IET Power Electronics*, vol. 5, no. 2, pp. 158–165, 2012. DOI: 10.1049/iet-pel.2011.0098.

[7] Zhe Li, Xi Zhang, Wei Qian, Hua Bai, "A novel zero-current-transition PWM DC-DC converter with coupled inductor", *IEEE 7th Int. Symposium on Power Electronics for Distributed Generation Systems (PEDG 2016)*, Vancouver, BC, 2016, pp. 1–4. DOI: 10.1109/PEDG.2016.7527021.

[8] V. Venkata Subrahmanya Kumar Bhajana, D. Pavel, "Design and experimental investigations on a new non-isolated zcs bidirectional buck-boost dc-dc converter for energy storage systems", *Rev. Roum. Sci. Techn. – Électrotechn. et Énerg*., vol. 60, no. 1, pp. 79–88, 2016.

[9] M. R. Mohammadi, H. Farzanehfard, "A new family of zero-voltage-transition nonisolated bidirectional converters with simple auxiliary circuit", *IEEE Trans. Industrial Electronics*, vol. 63, no. 3, pp. 1519–1527, 2016. DOI: 10.1109/TIE.2015.2498907.

[10] L. Sun, F. Zhuo, F. Wang, T. Zhu, "A non-isolated bidirectional soft-switching power-unit-based DC-DC converter with unipolar and bipolar structure for DC networks interconnection", *IEEE Trans. Industry Applications*, vol. 99, pp. 1–1. 2018. DOI: 10.1109/TIA.2018.2797256.